

Enthalpy relaxation behaviour of Al–Si–Cr quasicrystalline and amorphous alloys upon annealing

A. INOUE, A. P. TSAI*, H. M. KIMURA, T. MASUMOTO

*The Research Institute for Iron, Steel and Other Metals, and *Graduate School, Department of Material Science and Engineering, Tohoku University, Sendai 980, Japan*

Annealing-induced enthalpy relaxation behaviour was examined calorimetrically in quasicrystalline $\text{Al}_{62}\text{Si}_{19}\text{Cr}_{19}$ and amorphous $\text{Al}_{60}\text{Si}_{25}\text{Cr}_{15}$ alloys. When both alloys annealed at temperatures below T_x are reheated, an excess endothermic reaction (enthalpy relaxation) occurs reversibly above the annealing temperature, T_a . The peak temperature of $\Delta C_{p,\text{endo}}$ rises in a continuous manner with the logarithm of annealing time (t_a). The magnitudes of $\Delta C_{p,\text{endo}}$ and ΔH_{endo} of the amorphous alloy increase with increasing T_a while no appreciable change in $\Delta C_{p,\text{endo}}$ and ΔH_{endo} of the quasicrystal with T_a is seen. The activation energy, Q_m , for the enthalpy relaxation increases from 1.8 to 2.7 eV with the peak temperature of ΔC_p , T_m , for the amorphous alloy, whereas it remains constant (≈ 1.3 eV) for the quasicrystal. The endothermic reaction with small Q_m for the quasicrystal is thought to be attributable to the disappearance of short-range ordering of chromium and silicon atoms with stronger attractive interaction, which developed during annealing, i.e. the reversion phenomenon, in the unrelaxed localized regions with high free-energy isolately embedded in the more stable icosahedral structure. The similarity of the enthalpy relaxation behaviour between the quasicrystalline and amorphous phases allows us to infer that short-range atomic configuration is very similar between the quasicrystalline and amorphous phases.

1. Introduction

Since an icosahedral quasicrystal with long-range orientation order and quasiperiodicity inconsistent with periodic translational order was discovered in a rapidly quenched $\text{Al}_{85.7}\text{Mn}_{14.3}$ alloy [1], the quasicrystal has attracted rapidly increasing interest from the scientific point of view. Only in the last two years, have a number of quasicrystals been prepared by various techniques such as melt quenching, sputter deposition, solid state reaction and electron irradiation, etc. Additionally, many discussions have been presented on the growth of the icosahedral phase including the generation of disorder for a three-dimensional Penrose tiling in a realistic growth process which would have matching-rule violations [2].

Nelson and Halperin [3] pointed out a possible structural similarity between quasicrystal and metallic glasses; both the phases consist of the fundamental unit of an icosahedron. Additionally, Chen and co-workers [4, 5] have examined calorimetrically the structural stability of an $\text{Al}_{86}\text{Mn}_{14}$ quasicrystal and reported that the quasicrystal exhibits a reversible endothermic reaction upon heating the annealed sample, in addition to the heating-induced irreversible exothermic reaction at temperatures well below the icosahedral–orthorhombic transition. Their reactions are very similar to those for an amorphous alloy, suggesting the similarity of the short-range atomic configuration between quasicrystalline and amorphous

alloys. However, the rapidly quenched $\text{Al}_{86}\text{Mn}_{14}$ consists of the duplex phases of quasicrystal and aluminium and hence the reversible endothermic reaction might be due to the recoverable reaction of crystalline aluminium phase. In order to clarify the phenomenon and mechanism of enthalpy relaxation for the quasicrystal, it is essential to use a single-phase quasicrystal. Very recently, Inoue *et al.* [6] have found that a quasicrystal with mostly single phase is formed in rapidly quenched Al–Si–Cr alloys containing 20 at % Cr and 20 at % Si. The ternary alloys appear to be appropriate as the test sample to study the annealing-induced enthalpy relaxation because the irreversible and reversible enthalpy relaxations of an amorphous phase are much larger for the multicomponent systems containing more than three constituent elements, rather than for binary system. The aim of this paper is to examine the enthalpy relaxation behaviour of a quasicrystalline $\text{Al}_{62}\text{Si}_{19}\text{Cr}_{19}$ alloy, in comparison with that of an amorphous $\text{Al}_{60}\text{Si}_{25}\text{Cr}_{15}$ alloy, and to investigate the difference in the enthalpy relaxation behaviour between quasicrystalline and amorphous alloys.

2. Experimental procedures

Al–Si–Cr master ingots with composition $\text{Al}_{62}\text{Si}_{19}\text{Cr}_{19}$ and $\text{Al}_{60}\text{Si}_{25}\text{Cr}_{15}$ were prepared by arc melting a mixture of pure aluminium (99.99 wt %), chromium (99.75 wt %) and silicon (99.999 wt %) in a purified

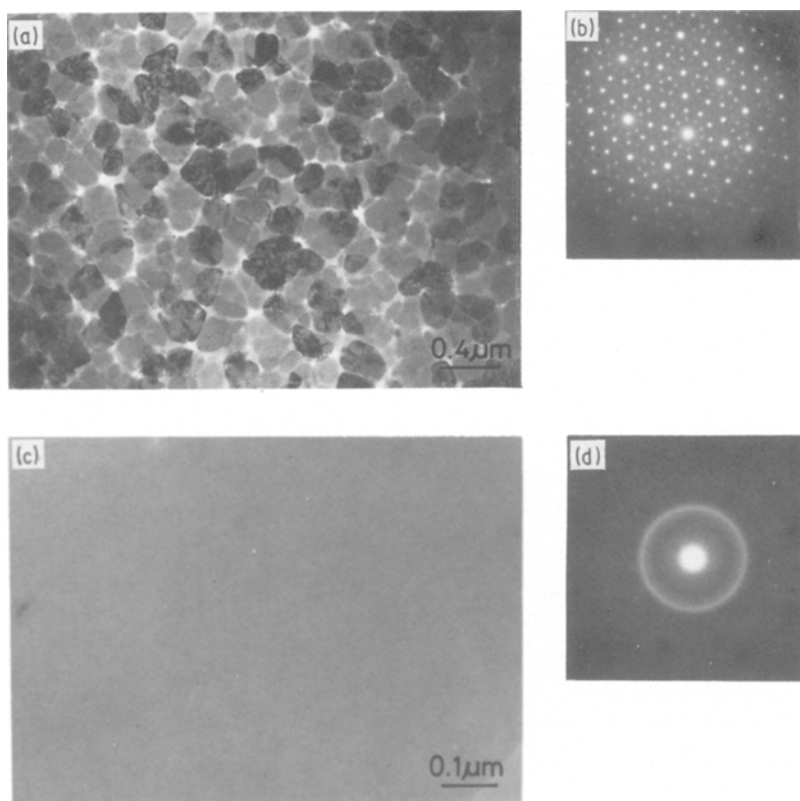


Figure 1 Bright-field electron micrographs and selected-area diffraction patterns of rapidly quenched $\text{Al}_{62}\text{Si}_{19}\text{Cr}_{19}$ (a and b) and $\text{Al}_{60}\text{Si}_{25}\text{Cr}_{15}$ (c and d) alloys.

argon atmosphere. Rapidly quenched ribbon specimens, about 0.02 mm thick and about 1 mm wide, were prepared from the master alloys under an argon atmosphere using a single-roller melt-spinning apparatus. The as-quenched structure was examined by conventional X-ray diffractometry and transmission electron microscopy (TEM). Thin foils for TEM were prepared by electrolytic polishing in an electrolyte of perchloric acid and ethanol with 1 : 9 volumetric ratio. The apparent specific heat, C_p , was measured with a differential scanning calorimeter (Perkin–Elmer DSC-II). Care was taken to reduce the thermal drift by prewarming the calorimeter for at least 5 h in the temperature of interest. The accuracy of the data was about $0.4 \text{ J mol}^{-1} \text{ K}^{-1}$ for the absolute C_p values, but was better than $0.2 \text{ J mol}^{-1} \text{ K}^{-1}$ for relative C_p or ΔC_p measurement. The as-quenched samples were subjected to annealing treatments at various temperatures ($T_a = 400$ to 550 K) for different periods ($t_a = 3$ to 200 h). Short-period anneals ($t_a \leq 12 \text{ h}$) were performed directly inside the calorimeter while long-duration anneals (48 to 200 h) were performed in a well-controlled furnace after placing the encapsulated samples inside a vacuum-sealed quartz tube. Following the annealing treatment, the sample was thermally scanned at 40 K min^{-1} from 320 to 680 K for the quasicrystal and from 320 to 600 K for the amorphous alloy to determine the $C_{p,a}$ of the annealed sample. It was then cooled to 320 K , and reheated immediately to obtain the $C_{p,s}$ data of the “reference” sample. This test procedure is essential in order to eliminate any possible error that might result from the drift in the calorimeter due to the prolonged annealing time between the measurements. This change in the calorimetric behaviour with annealing was used to monitor the enthalpy relaxation process.

3. Results

3.1. Quasicrystalline structure

Fig. 1 shows bright-field electron micrographs and selected-area diffraction patterns of rapidly quenched $\text{Al}_{62}\text{Si}_{19}\text{Cr}_{19}$ (a and b) and $\text{Al}_{60}\text{Si}_{25}\text{Cr}_{15}$ (c and d) alloys. $\text{Al}_{62}\text{Si}_{19}\text{Cr}_{19}$ consists of spherulitic grains with size of about 0.2 to $0.3 \mu\text{m}$. The electron diffraction pattern (b) shows five-fold symmetry which can be identified as an icosahedral structure. Fig. 2 shows an X-ray diffraction pattern as a function of diffraction angle for a rapidly quenched $\text{Al}_{62}\text{Si}_{19}\text{Cr}_{19}$ alloy. Identification of the X-ray diffraction peaks corresponding to the quasicrystal with an icosahedral structure was made by using six independent Miller indices as proposed by Bancel *et al.* [7]. As indexed in Fig. 2, the diffraction pattern of $\text{Al}_{62}\text{Si}_{19}\text{Cr}_{19}$ alloy consists mainly of quasicrystalline phase. Therefore, the X-ray data also allow us to conclude that mostly single phase with quasicrystal structure is formed in the vicinity of 19% Si and 19% Cr.

3.2. $C_p(T)$ and $\Delta C_p(T)$ behaviour of as-quenched samples

Fig. 3 shows the thermograms of the amorphous alloy in the as-quenched state. The C_p value of the as-quenched phase is about $23.0 \text{ J mol}^{-1} \text{ K}^{-1}$ near room temperature. As the temperature increases, the C_p value begins to decrease, indicative of a structural relaxation at about 365 K and increases gradually to $38 \text{ J mol}^{-1} \text{ K}^{-1}$ up to about 600 K . The difference in the $C_{p,s}$ and $C_{p,q}$ values represents an irreversible structural relaxation resulting from the annihilation of quenched-in “defects” and the development of topological and compositional short-range orderings.

Similar thermograms are obtained for the quasicrystalline alloy as shown in Fig. 4. In the comparison

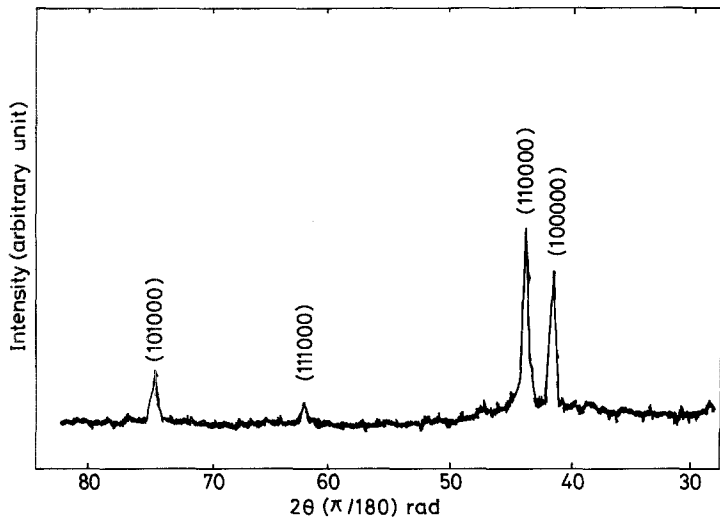


Figure 2 X-ray diffraction pattern as a function of diffraction angle for a rapidly quenched $\text{Al}_{62}\text{Si}_{19}\text{Cr}_{19}$ alloy.

of the $C_p(T)$ behaviour between the quasicrystalline and amorphous alloys, the difference is summarized as follows: (1) the temperature at which the exothermic reaction corresponding to an irreversible enthalpy relaxation begins to occur is higher by about 20 K for the quasicrystal than that for the amorphous alloy; (2) the temperature dependence of $C_{p,s}$ for the quasicrystal is smaller than that for the amorphous alloy; (3) the maximum value of structural relaxation represented by the difference between $C_{p,s}$ and $C_{p,q}$ is considerably larger for the amorphous alloy and the temperature at which the maximum structural relaxation occurs is much lower for the amorphous alloy, and (4) the crystallization temperature T_x for the quasicrystalline and amorphous alloys is 680 and 600 K, respectively, being higher for the quasicrystal. The irreversible relaxation of the quasicrystal is thought to be due to an annihilation of quenched-in "defects", a reduction of misfit strain and frustration, and a local rearrangement of aluminium, chromium and silicon atoms from a quenched-in unrelaxed state to a relaxed state.

Fig. 5 shows the temperature dependence of the difference in C_p between as-quenched and annealed states, $\Delta C_{p,exo}(T)$, for the quasicrystalline and amorphous alloys. The maximum magnitude of $\Delta C_{p,exo}(T)$

for the latter is larger by about 23% than that for the former. Furthermore, $\Delta H_{exo} \equiv (\int \Delta C_p dT)$ for the amorphous alloy (968 J mol^{-1}) is larger by about 15% than that (831 J mol^{-1}) for the quasicrystalline alloy. The peak temperature at which the magnitude of $\Delta C_{p,exo}(T)$ shows a maximum value is 666 K for the quasicrystal and 572 K for the amorphous alloy. These results indicate clearly that the irreversible structural relaxation upon heating occurs more easily even at low temperatures for the amorphous alloy and the thermal instability in their nonequilibrium structures is much higher for the amorphous alloy.

3.3. $C_p(T)$ and $\Delta C_p(T)$ behaviour of annealed samples

Figs 6 and 7 show the change in the thermograms, $C_{p,a}(T)$ of quasicrystalline and amorphous alloys with annealing temperature (T_a) and annealing time (t_a) for quasicrystalline $\text{Al}_{62}\text{Si}_{19}\text{Cr}_{19}$ and amorphous $\text{Al}_{60}\text{Si}_{25}\text{Cr}_{15}$ alloys. The data of the as-quenched samples are also shown for reference. $C_{p,a}$ shows a $C_p(T)$ behaviour which closely follows the specific heat curve of the reference sample, $C_{p,s}$, up to each T_a , and exhibits an excess endothermic peak relative to the reference sample before merging with that of the

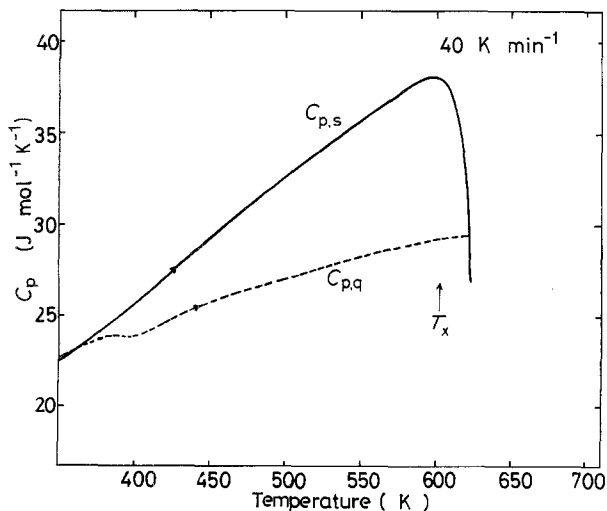


Figure 3 The thermogram of an amorphous $\text{Al}_{60}\text{Si}_{25}\text{Cr}_{15}$ alloy in the as-quenched state. The solid line presents the thermogram of the sample subjected to heating to 600 K.

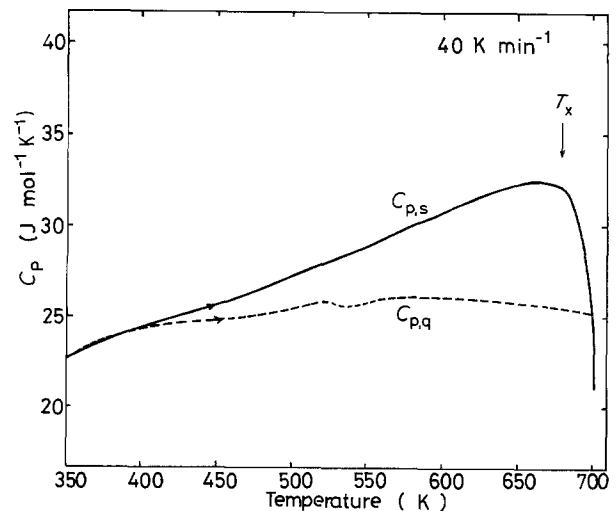


Figure 4 The thermogram of a quasicrystalline $\text{Al}_{62}\text{Si}_{19}\text{Cr}_{19}$ alloy in the as-quenched state. The solid line presents the thermogram of the sample subjected to heating to 680 K.

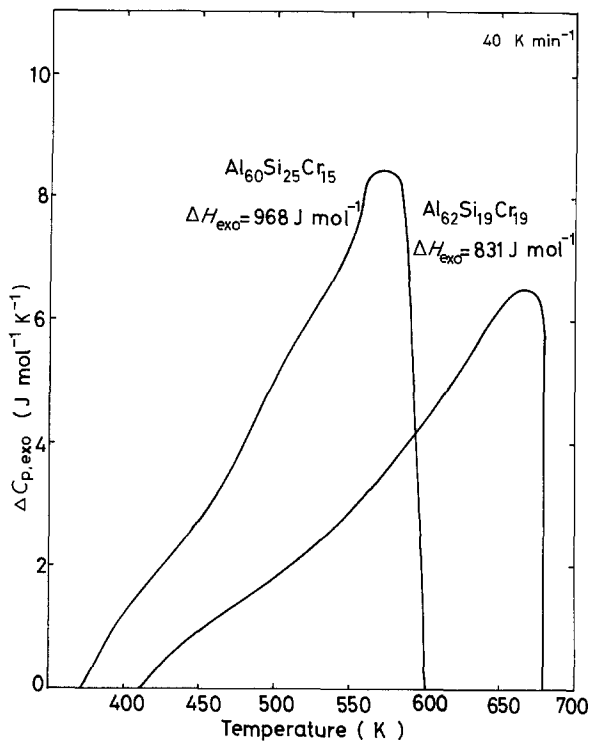


Figure 5 Difference in the specific heat between the as-quenched and annealed states ($\Delta C_{p,exo}$) against temperature for quasicrystalline $Al_{62}Si_{19}Cr_{19}$ and amorphous $Al_{60}Si_{25}Cr_{15}$ alloys.

as-quenched sample. The features of Figs 6 and 7 are:

1. The samples annealed at T_a show an excess endothermic reaction beginning at T_a , implying that the $C_{p,a}$ curve in the temperature range above T_a is dependent on the thermal history and consists of configura-

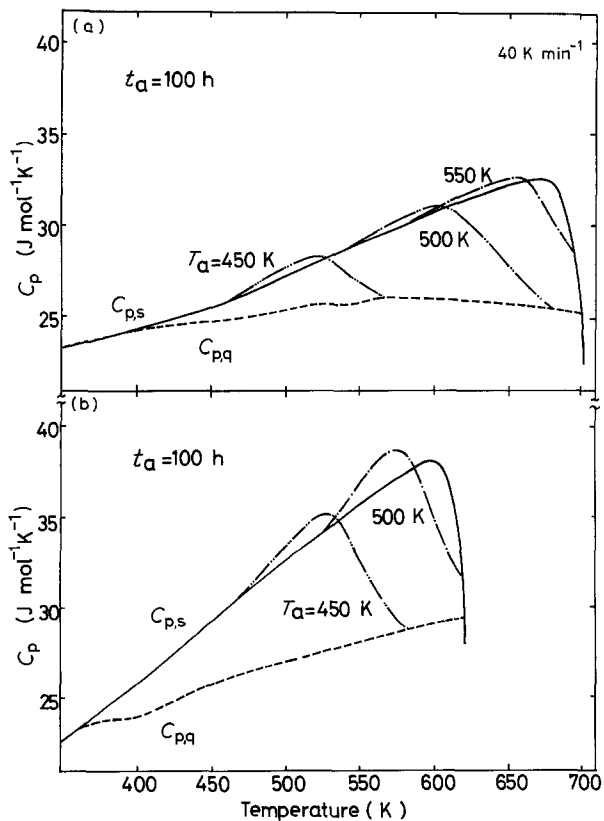


Figure 6 The thermograms of (a) quasicrystalline $Al_{62}Si_{19}Cr_{19}$ and (b) amorphous $Al_{60}Si_{25}Cr_{15}$ alloys subjected to annealing for 100 h at various temperatures ranging from 450 to 550 K. The solid lines represent the thermograms of the sample subjected to heating for 1 min at 680 and 600 K.

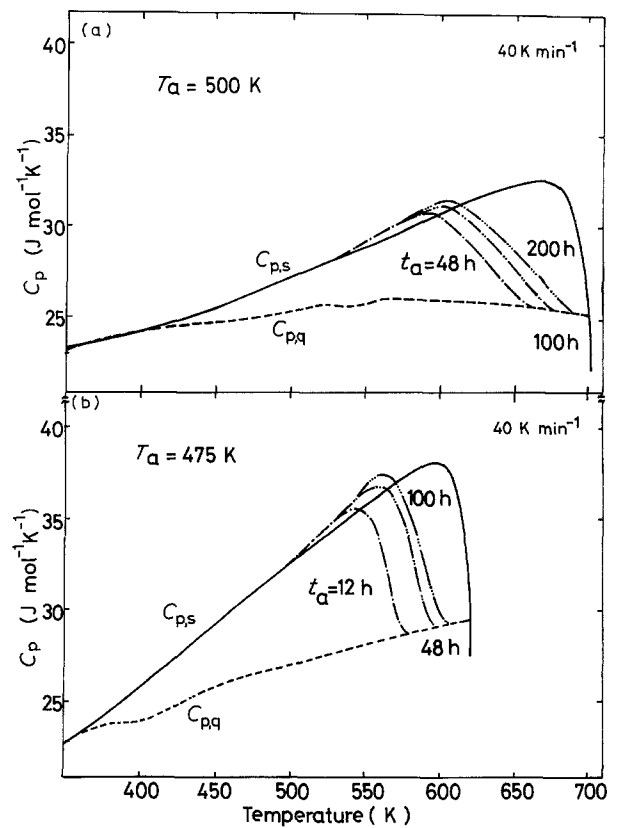


Figure 7 The thermograms of (a) quasicrystalline $Al_{62}Si_{19}Cr_{19}$ and (b) amorphous $Al_{60}Si_{25}Cr_{15}$ alloys subjected to annealing at 475 and 500 K for various periods from 12 to 200 h. The solid lines represent the thermograms of the sample subjected to heating for 1 min at 680 and 600 K.

tion contributions as well as those arising from purely thermal vibrations. Therefore, the vibrational specific heat $C_{p,v}$ for these two alloys was extrapolated from C_p values in the temperature region below 450 K and is linear function of temperature such that

$$C_{p,v} = 25.6 + 3.3 \times 10^{-2} (T - 450) \text{ J mol}^{-1} \text{ K}^{-1} \quad (1)$$

for the quasicrystalline alloy,

$$C_{p,v} = 29.2 + 5.7 \times 10^{-2} (T - 450) \text{ J mol}^{-1} \text{ K}^{-1} \quad (2)$$

for the amorphous alloy.

2. The excess endothermic curves of both the quasicrystalline and amorphous alloys always begin to rise at T_a , being independent of t_a . Furthermore, both the magnitude and the temperature of the endothermic peak tend to increase linearly with $\ln t_a$ as plotted in Fig. 8a for the quasicrystalline alloy and Fig. 8b for the amorphous alloy. The change in the temperature of the endothermic peak (T_m) with t_a is considerably larger for the amorphous alloy than for the quasicrystal.

3. The $\Delta C_{p,endo}(T)$ and $\Delta C_{p,exo}(T)$ behaviour for the quasicrystalline alloy are similar to those for the amorphous alloy. The excess endothermic peak is reversible while the exothermic broad peak is irreversible and the $C_p(T)$ curve of the annealed samples couples the reversible endothermic and irreversible exothermic reaction.

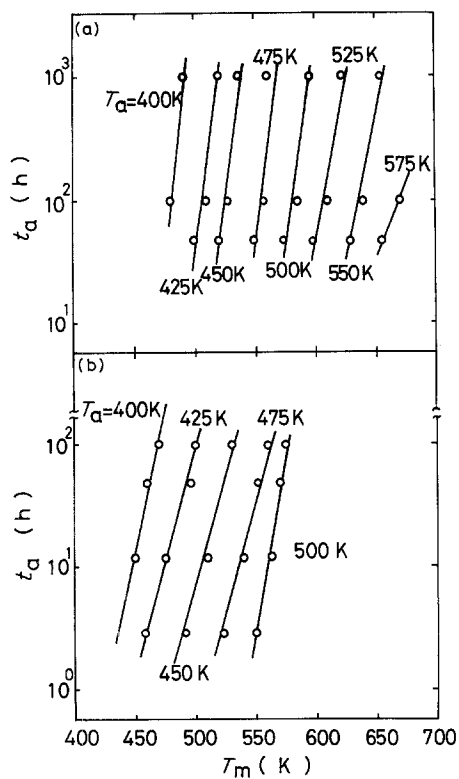


Figure 8 The variation of the $\Delta C_{p,endo}(=C_{p,a} - C_{p,s})$ peak temperature, T_m , as a function of annealing time, t_a , for (a) quasicrystalline $Al_{62}Si_{19}Cr_{19}$ and (b) amorphous $Al_{60}Si_{25}Cr_{15}$ alloys annealed at various temperatures from 400 to 575 K.

From the features derived from Figs 6 and 7, it is noted that the amorphous alloy exhibits a temperature dependence of $C_{p,a}$ ($5.7 \times 10^{-2} J mol^{-1} K^{-2}$) larger than that ($3.3 \times 10^{-2} J mol^{-1} K^{-2}$) of the quasicrystalline alloy, implying that internal structural change upon annealing is more sensitive for the amorphous alloy than for the quasicrystal. In other words, the thermal stability of the quasicrystalline structure is higher than that of the amorphous alloy. It has been suggested [8] for an amorphous alloy that reversible relaxation arises from compositional short-range localized relaxation of the more or less rigid matrix while the irreversible structural relaxation results from the annihilation of various kinds of quenched-in defects as well as the topological and compositional atomic regroupings. The exothermic reaction in the quasicrystalline alloy may be attributed to the same

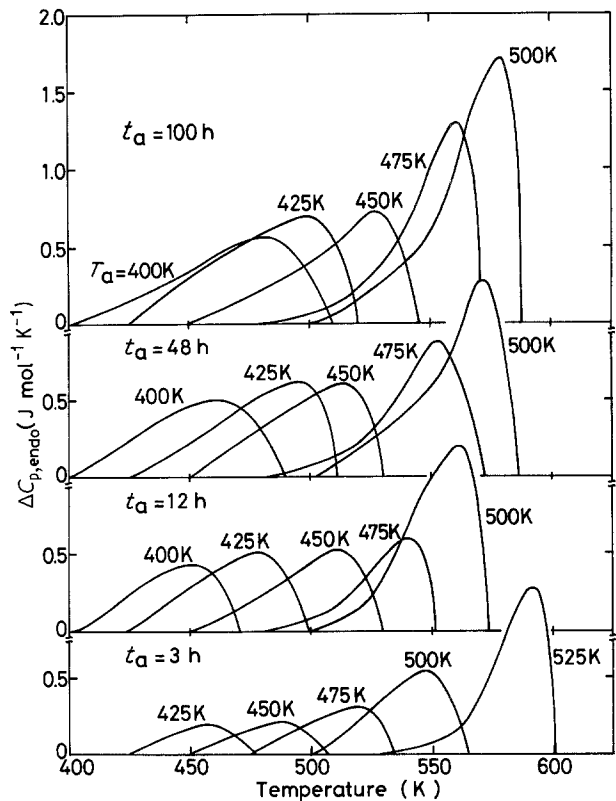


Figure 9 The differential specific heat, $\Delta C_{p,endo}(T)$, between the reference and annealed samples for an amorphous $Al_{60}Si_{25}Cr_{15}$ alloy subjected to annealing at various temperatures ranging from 400 to 525 K for different periods from 3 to 100 h.

reason as that in an amorphous alloy. More detailed discussion of this point will be given below.

3.4. Changes in $\Delta C_{p,endo}$ and ΔH_{endo} with T_a and t_a

The change in the difference of specific heat $\Delta C_{p,endo} = (C_{p,a} - C_{p,s})$ for the samples annealed for different periods at different temperatures is shown in Fig. 9 for the amorphous alloy and Fig. 10 for the quasicrystal. As replotted as a function of T_a in Fig. 11, with increasing T_a , the $\Delta C_{p,endo}$ of the amorphous alloy increases gradually followed by a rapid increase at $T_a \approx 500$ K, similar to the result for many other amorphous alloys [9]. On the other hand, $\Delta C_{p,endo}$ of the quasicrystal is independent of T_a . The difference of the change in $\Delta C_{p,endo}$ with T_a between the two alloys

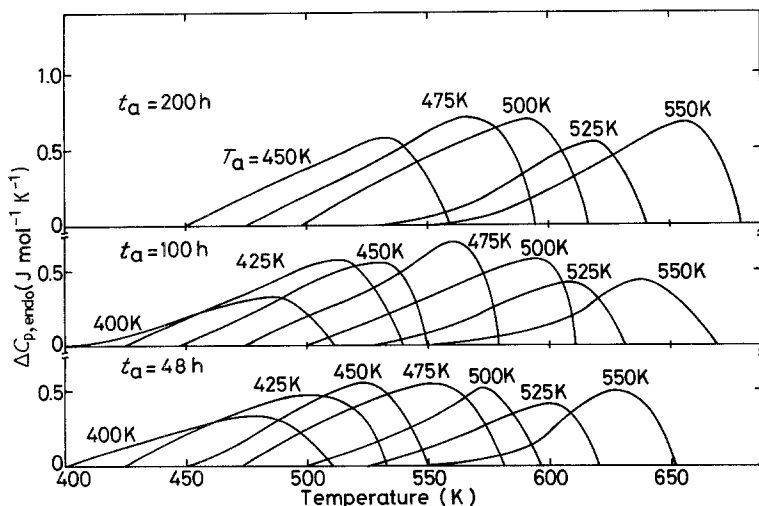


Figure 10 The differential specific heat, $\Delta C_{p,endo}(T)$, between the reference and annealed samples for a quasicrystalline $Al_{62}Si_{19}Cr_{19}$ alloy subjected to annealing at various temperatures ranging from 400 to 550 K for different periods from 48 to 200 h.

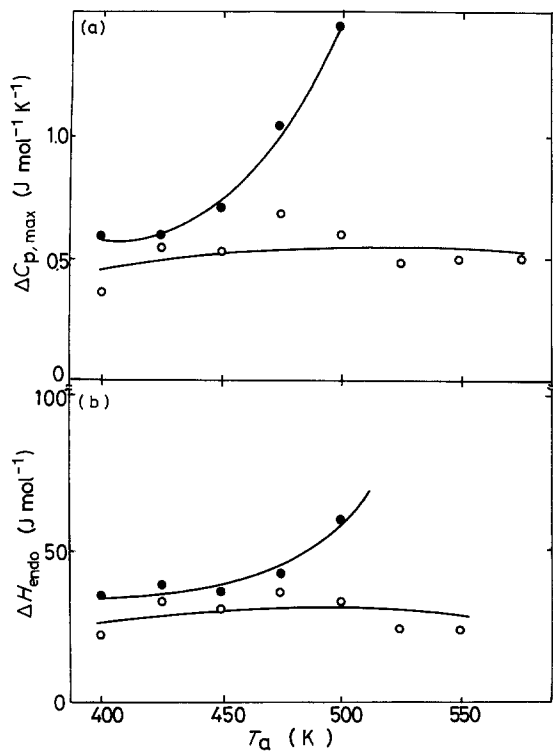


Figure 11 The variations of (a) the maximum differential specific heat, $\Delta C_{p,\max}$, and (b) the enthalpy relaxation, ΔH_{endo} , as a function of annealing temperature, T_a , for (●) amorphous $\text{Al}_{60}\text{Si}_{25}\text{Cr}_{15}$ and (○) quasicrystalline $\text{Al}_{62}\text{Si}_{19}\text{Cr}_{19}$ alloys subjected to annealing for 100 h.

suggests that the distribution of annealing-induced relaxation entity as a function of temperature is not always the same in the amorphous and the quasicrystalline phases.

Fig. 12 shows the changes in $\Delta C_{p,\max}$ and ΔH_{endo} as a function of t_a at $T_a = 475$ and 500 K for the amorphous alloy and the quasicrystal. Here

$$\Delta H_{\text{endo}}(T_a, t_a) = \int \Delta C_p(T) (= C_{p,a} - C_{p,s}) dT \quad (3)$$

$\Delta C_p(T) \geq 0$

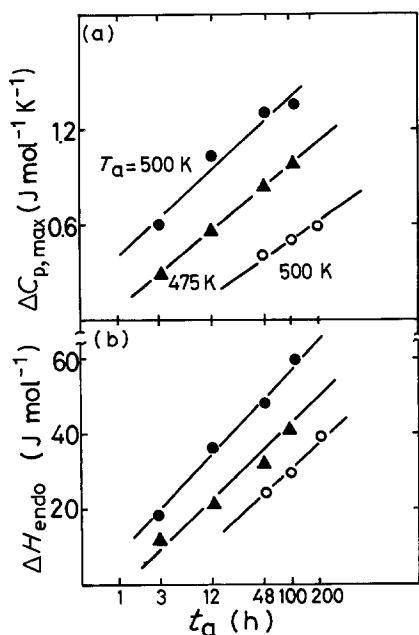


Figure 12 The variations of (a) the maximum differential specific heat, $\Delta C_{p,\max}$, and (b) the enthalpy relaxation, ΔH_{endo} , as a function of annealing time, t_a , for (○) quasicrystalline $\text{Al}_{62}\text{Si}_{19}\text{Cr}_{19}$ and (●, ▲) amorphous $\text{Al}_{60}\text{Si}_{25}\text{Cr}_{15}$ alloys at 475 and 500 K.

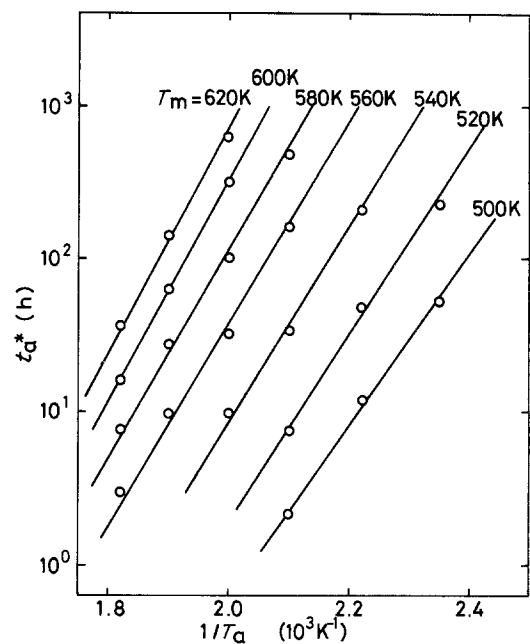


Figure 13 The annealing time, t_a^* , for the appearance of the $\Delta C_{p,\max}$ peak at T_m as a function of the inverse of the annealing temperature, $1/T_a$, for a quasicrystalline $\text{Al}_{62}\text{Si}_{19}\text{Cr}_{19}$ alloy.

$\Delta C_{p,\max}$ and ΔH_{endo} of both alloys increase almost linearly with $\ln t_a$ in an annealing time less than 200 h.

4. Discussion

4.1. Activation energy for enthalpy relaxation

$$Q_m(T_m)$$

The activation energy for structural relaxation can be estimated from the changes of T_m by isothermal annealing. If the $\Delta C_{p,\text{endo}}$ peak at T_m is associated with a relaxation entity, an apparent activation energy for enthalpy relaxation, Q_m , of the amorphous and quasicrystalline alloys can be evaluated from isothermal annealing data of Fig. 7 by using the following relation [10]

$$Q(T_m)/k_B = d \ln t_a^*/d(1/T_a) \quad (4)$$

where t_a^* is the annealing time for the appearance of $\Delta C_{p,\max}$ at T_m and k_B is Boltzmann's constant. A rather good linearity in the Arrhenius relation for each peak is seen in Fig. 13 and the Q_m value can be estimated. As plotted in Fig. 14, $Q_m(T_m)$ of the amorphous alloy is not constant and increases with increasing T_m from 1.8 eV at $T_m = 460$ K to 2.5 eV at $T_m = 560$ K, while that of the quasicrystal is almost independent of T_m and remains constant (about 1.3 eV). Thus, Q_m is much larger for the amorphous alloy over the whole T_m range. In general, Q_m of an amorphous alloy increases drastically at the glass transition and/or at temperatures just below crystallization temperature. Accordingly, the smaller $Q_m(T_m)$ values and the independent behaviour of Q_m with T_m for the quasicrystalline alloy reflect structural relaxation in a very localized region which is independent of temperature, while the larger $Q_m(T_m)$ values and the strong dependence on temperature for the amorphous alloy reflect local- and medium- (or long-) range structural relaxation at temperatures well and just below T_x , respectively.

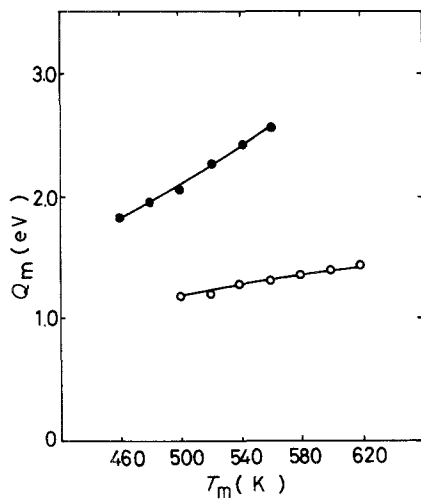


Figure 14 The activation energy spectrum $Q_m(T_m)$ as a function of T_m for (○) quasicrystalline $\text{Al}_{62}\text{Si}_{19}\text{Cr}_{19}$ and (●) amorphous $\text{Al}_{60}\text{Si}_{25}\text{Cr}_{15}$ alloys.

4.2. Distribution of annealing-induced relaxation entity, $N_0(T)$

In a previous section, the activation energy for enthalpy relaxation was demonstrated to have a broad distribution with T_m . Based on Primak's theory [11] on the kinetics of processes distributed in activation energy, the enthalpy relaxation spectrum as a function of T_m has been evaluated by Chen and Crest [12]. According to their analysis, the relation $\Delta C_{p,\text{endo}}(T)$ is evaluated from Equation 5

$$\Delta C_{p,\text{endo}}(T) = N_0(T)\gamma(T) \quad (5)$$

where $N_0(T)$ is the distribution of the relaxation entity, and $\gamma(T)$ is the coupling strength contribution to the specific heat $\Delta C_{p,\text{endo}}$. As $\gamma(T) \propto (T - T_a)$, Equation 5 reduces to

$$N_0(T) \propto \Delta C_{p,\text{endo}}(T)/(T - T_a) \quad (6)$$

$N_0(T)$ values of the amorphous and quasicrystalline alloys evaluated from leading edges of $\Delta C_{p,\text{endo}}(T)$ shown in Figs 9 and 10 are plotted in Fig. 15. It is seen that $N_0(T)$ shows a rapid increase near T_x for the amorphous alloy while $N_0(T)$ of the quasicrystal remains unchanged with temperature. It is thus con-

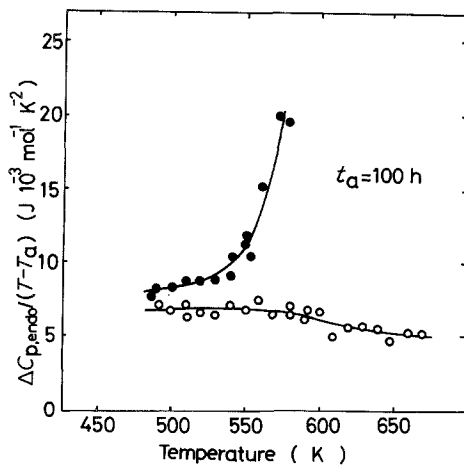


Figure 15 The relaxation entity spectra $N_0(T) = \Delta C_{p,\text{endo}}(T)/(T - T_a)$ for (○) quasicrystalline $\text{Al}_{62}\text{Si}_{19}\text{Cr}_{19}$ and (●) amorphous $\text{Al}_{60}\text{Si}_{25}\text{Cr}_{15}$ alloys as a function of temperature.

cluded that the N_0-T curves can reproduce fairly well the actually measured distribution of maximum $\Delta C_{p,\text{endo}}$ and ΔH_{endo} as a function of T_a shown in Figs 9, 10 and 11, because $T_m - T_a$ is nearly constant.

4.3. Interpretation of the reversible endothermic reaction in the quasicrystalline alloy

Before the interpretation of the reversible structural relaxation for the quasicrystal is presented, it appears valuable to explain the concept of the reversible structural relaxation for an amorphous alloy because the short-range structure in both phases has been thought to be quite similar, i.e. an icosahedral atomic configuration [4]. Cyat [13] and Chen [10] proposed that a supercooled liquid structure near T_g is inhomogeneous and consists of liquid-like regions of large free volume or high local free energy, and solid-like regions with small free volume or low local free energy. The resulting amorphous solid quenched from the liquid contains a large number of liquid-like regions with unrelaxed atomic configurations isolated from each other and embedded in the solid-like matrix. The inhomogeneity in the amorphous alloy is thought to arise from fluctuation in concentration and density. When the amorphous alloy is annealed at T_a for t_a , parts of the liquid-like regions undergo configurational changes to solid-like (i.e. relaxed structural state) in an independent and non-cooperative manner. However, the local structural relaxation in a cluster involving several atoms can be cooperative and the size of this cluster has been estimated to be less than 1 to 2 nm. Upon heating, reversion occurs above T_a and this initial amorphous structure is recovered. The effect of initial annealing is eliminated upon heating but will appear again upon repeated annealing. The effects of annealing are thus reversible and additive. As T_a increases, the solid-like (relaxed) cluster increases in number and grows in size to such an extent that a larger cluster is formed. The structural relaxation is then related to a percolation process [14]. The concept is in good agreement with the results shown in Figs 9, 12 and 15.

Recently, the relationship between the short-range icosahedral order in amorphous alloys and the long-range order in icosahedral crystals have been explored by Sachdev and Nelson [15]. They found that liquids near T_g are metastable with respect to a vertex-model icosahedron which is stabilized because the most prominent Bragg peaks are in appropriate registry with peaks in the liquid structure factor. Furthermore, Kofalt *et al.* [16] have investigated the structure of the amorphous and quasicrystalline $\text{Pd}_{60}\text{U}_{20}\text{Si}_{20}$ by X-ray diffraction and found that the distribution of atomic pairs in the amorphous phase is similar to that in the quasicrystalline phase on the scale of 0.6 nm, implying that the local structure between these two phases is quite similar. From the good similarity of the short-range atomic configuration, it may be considered that the icosahedral structure is the most important unit cell in metallic liquid or glass. Therefore, the icosahedral structure with a developed short-range ordering is regarded as a solid-like region with

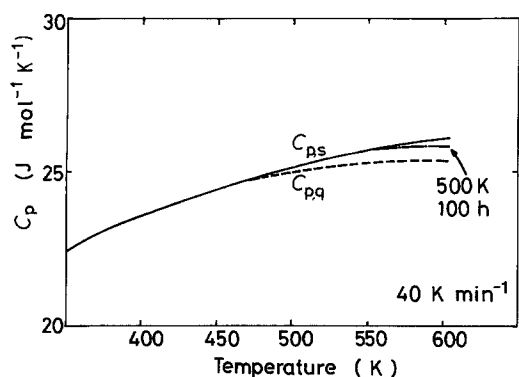


Figure 16 The thermograms of a quasicrystalline $\text{Al}_{84.6}\text{Cr}_{15.4}$ alloy subjected to annealing at 500 K for 100 h. The solid line represents the thermogram of the sample subjected to heating at 600 K for 1 min.

a close-packed cluster in an amorphous solid, even though a clear picture of the solid- and liquid-like regions remains unknown in the three-dimensional icosahedral structure consisting of two kinds of rhombohedra [17] where the sites of aluminium, chromium and silicon atoms are thought to be fixed. The similarity in the short-range atomic configuration between the amorphous and icosahedral phases allows us to use a similar concept to that proposed for an amorphous alloy in the interpretation of the enthalpy relaxation behaviour of the quasicrystal. Accordingly, the endothermic reaction for the quasicrystalline alloy may be attributed to an unrelaxed-relaxed transition in the icosahedral atomic configuration similar to liquid-solid-like transition in an amorphous alloy.

The following three experimental results on the enthalpy relaxation behaviour of some quasicrystalline alloys were found:

1. No endothermic reaction is detected in quasicrystalline $\text{Al}_{84.6}\text{Cr}_{15.4}$ [14] and $\text{Al}_{80}\text{Mn}_{20}$ [18] binary alloys, as exemplified for the Al-Cr alloy in Fig. 16.

2. The icosahedrons in quasicrystal have been considered to consist of two kinds of rhombohedra (types I and II) whose faces have "golden rhombuses" [17]. Additionally, the atomic sites in the quasilattice have been determined from high-resolution electron micrograph images for Al-Mn-Si alloys [19, 20]: as illustrated in Fig. 17, chromium occupies the vertices of the two rhombohedra and aluminium and silicon lie at two specified positions on the longest diagonal line in

the type I rhombohedron and at two specified positions on the diagonal line in all rhombic lateral faces in the types I and II rhombohedra. Furthermore, the existing probability has been estimated to be about 0.4 to 0.5 as represented by numbers in Fig. 17.

3. The interlattice spacing of quasicrystalline $\text{Al}_{62}\text{Si}_{19}\text{Cr}_{19}$ alloy is slightly smaller than that of quasicrystalline $\text{Al}_{84.6}\text{Cr}_{15.4}$ alloy because of the replacement of aluminium by silicon with a smaller atomic size.

The multiplication of the constituent atoms results in an increase in inhomogeneity in compositional density even in the quasicrystals. Accordingly, the endothermic reaction appears to be attributable to the difference in the bonding behaviour between chromium and silicon or aluminium atoms, probably because the difference in the bonding force becomes larger with increasing number of constituent elements. It is thought that the unrelaxed regions with a higher degree of inhomogeneity in quasicrystalline $\text{Al}_{62}\text{Si}_{19}\text{Cr}_{19}$ alloy have a disorder configuration between chromium and silicon or aluminium and are isolately embedded over a short range (smaller than that of amorphous phase) in the icosahedral matrix with an atomic configuration which is more rigid than that of an amorphous alloy. Each unrelaxed region undergoes configurational ordering resulting from the development of Cr-Si pairs which are thought to have the strongest attractive interaction from comparison [21] of hardness, melting temperature, decomposition temperature and heat of mixing among the compounds in Cr-Si, Al-Cr and Al-Si systems. The region is localized and the ordering is independent of each other or non-cooperative in nature upon annealing. The subsequent heating to a temperature above T_a results in the disappearance of the short-range compositional ordering (Cr-Si pairs) developed during annealing because of the increase in configurational entropy with increasing temperature, similar to the order-disorder transformation behaviour. A more detailed and systematic study on the structural relaxation is in progress for the quasicrystalline and amorphous phases in the rapidly quenched Al-Ge-Mn and Al-Ge-Cr alloys found very recently by Inoue *et al.* [22].

5. Conclusion

In order to clarify the annealing-induced relaxation

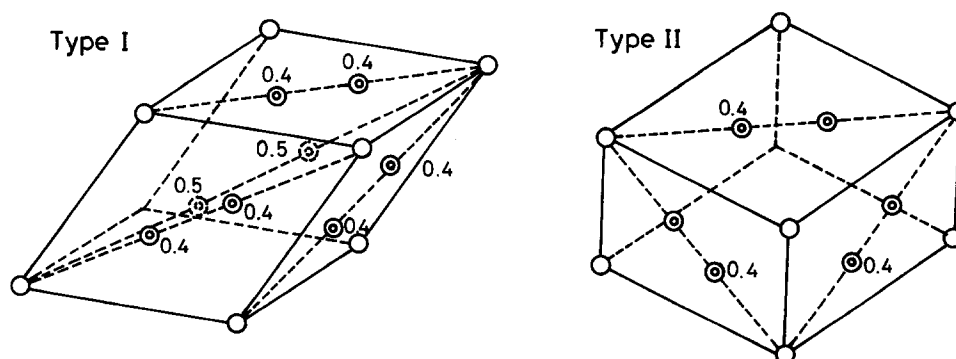


Figure 17 Fundamental unit cells (two kinds of rhombohedra) constructing a three-dimensional Penrose tiling and atomic site of the constituent elements. Each face of these rhombohedra consists of "golden rhombuses" where the ratio of the length of two diagonal lines has the "golden ratio" ($\tau = 1.618$). The numbers at each atomic site represent the existing probability of the atoms.

behaviour of a quasicrystal, the enthalpy change for an $\text{Al}_{62}\text{Si}_{19}\text{Cr}_{19}$ quasicrystal with an icosahedral structure has been investigated for samples annealed for different periods of 48 to 200 h in the temperature range 400 to 550 K, in comparison with that for an amorphous $\text{Al}_{60}\text{Si}_{25}\text{Cr}_{15}$ alloy with similar alloy composition. The results obtained are:

1. Upon heating the annealed samples, the quasicrystalline alloy as well as the amorphous alloy showed an excess endothermic reaction (enthalpy relaxation) above T_a followed by a broad exothermic reaction, and the endothermic reaction was reversible. The peak temperature of the endothermic reaction, $\Delta C_{p,\text{endo}}(T_m)$, increased almost linearly with $\ln t_a$.

2. The magnitude of the $\Delta C_{p,\text{endo}}$ peak for the quasicrystal is independent of T_a , being different from the results for the amorphous alloy in that it increases significantly with rising T_a . The activation energy for the enthalpy relaxation of the amorphous alloy increases with increasing temperature from 1.8 eV at 460 K to 2.60 eV at 550 K, while the quasicrystal has an activation energy of ≈ 1.3 eV, independent of temperature.

3. As no endothermic peak is seen in $\text{Al}_{84.6}\text{Cr}_{15.4}$ quasicrystal, the endothermic reaction in $\text{Al}_{62}\text{Si}_{19}\text{Cr}_{19}$ quasicrystal was attributed to the local-range rearrangement of chromium and silicon atoms in the fundamental units of two kinds of rhombohedra from a short-range ordered state developed during annealing to a disordered state, similar to the interpretation proposed in an amorphous alloy.

Interpretation of the annealing-induced relaxation behaviour of the Al–Si–Cr quasicrystal on the basis of a similar concept to that for an amorphous alloy is also supported from the experimental and theoretical evidence that the short-range structure is very similar in the quasicrystalline and amorphous phases in $\text{Pd}_{60}\text{U}_{20}\text{Si}_{20}$ alloy and in the quasicrystal and glass or liquid.

References

1. D. SHECTMAN, I. A. BLECH, D. GRATIAS and J. W. CAHN, *Phys. Rev. Lett.* **53** (1984) 1951.
2. V. ELSER, *ibid.* **54** (1985) 1730.
3. D. R. NELSON and B. I. HALPERIN, *Science* **229** (1985) 223.
4. H. S. CHEN and C. H. CHEN, *Phys. Rev. B* **33** (1986) 668.
5. H. S. CHEN, C. H. CHEN, A. INOUE and J. T. KRAUSE, *ibid.* **32** (1985) 1940.
6. A. INOUE, H. M. KIMURA and T. MASUMOTO, *J. Mater. Sci.* **22** (1987) 1864.
7. P. A. BANCEL, P. A. HEINEY, P. W. STEPHENS, A. I. GOLDMAN and P. M. HORN, *Phys. Rev. Lett.* **54** (1985) 2422.
8. A. INOUE, T. MASUMOTO and H. S. CHEN, *J. Mater. Sci.* **20** (1985) 2417.
9. A. INOUE, T. MASUMOTO and H. S. CHEN, *ibid.* **20** (1985) 4057.
10. H. S. CHEN, *J. Non-Cryst. Solids* **27** (1978) 257.
11. W. PRIMAK, *Phys. Rev.* **100** (1955) 1677.
12. M. H. CHEN and G. S. CREST, *Phys. Rev. B* **20** (1979) 1077.
13. M. CYAT, *J. Phys.* **C-8** (1980) 107.
14. K. K. SHANTE and S. KIRKPATRICK, *Adv. Phys.* **20** (1971) 325.
15. S. SACHDEV and D. R. NELSON, *Phys. Rev. B* **32** (1985) 4592.
16. D. D. KOFALT, S. NANAQ, T. EGAMI, K. M. WONG and S. J. POON, *Phys. Rev. Lett.* **57** (1986) 114.
17. T. OGAWA, *J. Phys. Soc. Jpn* **54** (1985) 3205.
18. A. INOUE, A. P. TSAI, H. M. KIMURA and T. MASUMOTO, unpublished research (1986).
19. K. HIRAGA, M. HIRABAYASHI, A. INOUE and T. MASUMOTO, *J. Electron Microscopy*, in press.
20. K. HIRAGA and S. YAMAMOTO, unpublished research (1986).
21. "Metals Databook", (Japan Institute of Metals, Maruzen, Tokyo, 1984).
22. A. INOUE, A. P. TSAI, H. M. KIMURA, Y. BIZEN and T. MASUMOTO, *J. Mater. Sci. Lett.* **6** (1987) 771.

Received 2 February
and accepted 15 April 1987